Mixture Boiling

Mark A. Kedzierski

Abstract

This chapter provides the engineer and the researcher with correlations and models for the prediction of the critical aspects of the boiling heat transfer of mixtures. This chapter offers a reliable, hands-on resource for solving common problems across pool boiling and flow boiling applications such as miscible mixtures, refrigerant/lubricant mixtures, additives, and refrigerant/nano-lubricants. Fundamental heat transfer and thermodynamic principles are succinctly provided to accompany the correlations and models. This chapter was written with the busy engineer in mind by providing simple but accurate prediction methods, and guidance where neither correlations nor models exist.

Nomenclature

English Symbols

a	surface area, m^2
A_c	cross-sectional flow area inside tube, m^2
A_n	coefficients given in Eq. (26)
A_i	actual inner surface area of tube, m^2
A_s	heat transfer surface area, m
b	fourth-degree polynomial in w_l, Eq. (27)
B_n	coefficients given in Eq. (26)
Bo	local boiling number, $\frac{q''}{G_r i_{fg}}$
c_p	specific heat, $J \cdot kg^{-1} \cdot K^{-1}$
c	fourth-degree polynomial in w_l, Eq. (27), K
C	coefficients given in Eqs. (16) and (32)
D	tube diameter, m

M.A. Kedzierski (✉)
National Institute of Standards and Technology, Gaithersburg, MD, USA
e-mail: MAK@nist.gov

F.A. Kulacki (ed.), *Handbook of Thermal Science and Engineering*,
DOI 10.1007/978-3-319-32003-8_44-1

D_e	equivalent inner diameter of smooth tube, $\sqrt{\frac{4A_c}{\pi}}$, m
D_h	hydraulic diameter of microfin tube, m
D_{np}	nanoparticle diameter, m
e	fin height, m
E	Reynolds number enhancement factor given in Eq. (13)
F	exponential constant in Eq. (1)
g	gravitational acceleration, $m{\cdot}s^{-2}$
G	total mass velocity, $kg{\cdot}m^{-2}{\cdot}s^{-1}$
h_{fg}	latent heat of vaporization, $kJ{\cdot}kg^{-1}$
h_i	ideal mixture heat transfer coefficient, $W{\cdot}m^{-2}\,K^{-1}$
h_m	heat transfer coefficient of refrigerant/lubricant mixture, $W{\cdot}m^{-2}\,K^{-1}$
$h_{2\phi}$	local two-phase heat-transfer coefficient, $W{\cdot}m^{-2}\,K^{-1}$
i_m	mass transfer coefficient, $m{\cdot}s^{-1}$
k	refrigerant thermal conductivity, $W{\cdot}m^{-2}\,K^{-1}$
K	mixture correction factor Eq. (15)
l_e	thickness of excess layer, m
l_a	thickness of adiabatic/Van der Waals excess layer, m
L	tube length, m
m	fitting constant in Eq. (32)
$\dot{m}$	mass flow rate, $kg{\cdot}s^{-1}$
M_w	molecular weight, $g{\cdot}mole^{-1}$
n_a	bubble site density, s^{-1}
Nu	local Nusselt number based on D_h
N_f	number of fins
N_{np}	the number of nanoparticles
N_{np}/A_s	nanoparticle surface density, m^{-2}
p	wetted perimeter, m
P	local fluid pressure, Pa
Pr	liquid refrigerant Prandtl number $\frac{c_p\mu}{k}\Big\vert_{r,l}$
q	heat duty, W
q''	local heat flux, $W{\cdot}m^{-2}$
q''_n	$= \frac{q''_{PL}}{1W{\cdot}m^{-2}}$
r_c	critical site radius for bubble nucleation, m
r_b	bubble departure radius, m
Re	all-liquid, refrigerant Reynolds number based on $D_h = \frac{G_r D_h}{\mu_{r,l}}$
s	spacing between the fins, m
S	suppression factor given in Eq. (14)
S_p	perimeter of one fin and channel, m
t_b	thickness of the fin at its base, m
t_w	thickness of the tube wall, m
T	temperature, K
T_b	bubble point temperature of mixture, K
T_c	refrigerant/lubricant critical solution temperature (lower limit), K

T_d	dew point temperature of mixture, K
T_{e}	temperature at excess layer/bulk fluid interface, K
T_{ib}	temperature of the liquid–vapor interface at bottom of tube, K
T_{it}	temperature of the liquid–vapor interface at top of tube, K
T_{w}	temperature at roughened surface, K
w	bulk lubricant mass fraction
x	mass fraction
x_{i}	mass fraction or mole fraction of ith component
x_{m}	mole fraction
x_q	thermodynamic mass quality
z	axial distance, m

Greek Symbols

α	helix angle between microfin and tube axis
β	fin-tip angle, radians
γ	surface free energy, $\mathrm{kg{\cdot}s^{-2}}$
Γ	excess surface density, $\mathrm{kg{\cdot}m^{-2}}$
ΔT_s	wall superheat: $T_{\mathrm{w}} - T_{\mathrm{s}}$, K
ΔT_{le}	temperature drop across excess layer, K
ζ	fraction of excess layer removed per bubble
θ	dimensionless thermal boundary layer temperature profile
Θ	bubble contact angle, rad
λ	thermal boundary constant
μ	dynamic viscosity $\mathrm{kg{\cdot}m^{-1}{\cdot}s^{-1}}$
ν	kinematic viscosity, $\mathrm{m^2{\cdot}s^{-1}}$
ρ	mass density of liquid, $\mathrm{kg{\cdot}m^{-3}}$
σ	liquid–vapor surface tension, $\mathrm{kg{\cdot}s^{-2}}$
ρ	density, $\mathrm{kg{\cdot}m^{-3}}$
ϕ	nanoparticle volume fraction
χ_{tt}	Lockhart–Martinelli parameter $((1 - x_{\mathrm{q}})/x_{\mathrm{q}})^{0.9}(\rho_{\mathrm{v}}/\rho_{\mathrm{l}})^{0.5}(\mu_{\mathrm{l}}/\mu_{\mathrm{v}})^{0.1}$
Ψ	sphericity

Subscripts

1	system 1
2	system 2
A	additive
b	bulk condition, fin base
c	critical condition
f	water
G	surface geometry dependent
i	inner
l	liquid, local
L	pure lubricant without nanoparticles
LV	least volatile component
m	mixture

mb	mixture boiling
MV	more volatile component
nL	nanolubricant
np	refrigerant/nanolubricant
p	plain or smooth tube, predicted
pL	refrigerant/nanolubricant
r	refrigerant
s	saturated state
v	vapor
w	heat transfer surface

Contents

1 Introduction

Mixture boiling has been practiced since antiquity. The ancient Greeks made their drinking water by distilling sea water. In the nineteenth century, oil was refined by distillation to make kerosene for lamps. Although the practical application of mixture heat transfer is very old, the experimental and theoretical study of it is relatively new. During this short period of study, researchers have found that liquid mixtures do not always evaporate as efficiently as single component liquids (Thome 1990; Shock 1982).

Mixtures can be completely miscible liquids of similar properties, like mixtures of refrigerants, or they can be mixed components that can have very different properties like nanofluids, refrigerant/lubricant mixtures, or colloids of immiscible liquids. Nanofluids are liquids mixed with well-dispersed nanoparticles. Typically, nanofluids have nanoparticles of 200 nm or less. Water-based nanofluids are water

suspensions with nanoparticles. Nanolubricants are lubricant-based suspensions with nanoparticles. Refrigerant/nanolubricants have been recently investigated for their potential to improve refrigerant/lubricant boiling performance. Refrigerant mixtures have been of high interest in recent years as they have begun to replace refrigerants with high ozone depletion potential and high global warming potential (Brown 2013).

Certain trade names and company products are mentioned in the text or identified in an illustration in order to adequately specify the experimental procedure and equipment used. In no case does such an identification imply recommendation or endorsement by the National Institute of Standards and Technology, nor does it imply that the products are necessarily the best available for the purpose.

2 Mixture Properties

Miscible mixture boiling is governed by the same physics as single-component boiling with two additional complications. The first complication is that the thermodynamic and the transport properties of a mixture typically cannot be predicted by averaging the constituent pure component properties (Kedzierski et al. 1992). The prediction of mixture thermodynamic properties requires an equation of state with interaction parameters. The interaction parameters are fluid pair dependent and may also vary with composition (Lemmon et al. 2013). The second complication is that heat transfer induces temperature gradients that can cause composition gradients within the liquid phase. In addition, differences between the liquid and vapor phase compositions may also exist.

Composition gradients may lead to mass transfer resistance, which degrades heat transfer (Shock 1982). How the composition differences influence heat transfer must be considered and predicted. Some mixtures do not exhibit differences in composition between the liquid and vapor phases. These mixtures are called azeotropes. Once the properties are correctly calculated, single-component models can be used to predict the heat transfer performance of azeotropic mixtures. Zeotropic mixtures are mixtures with composition differences between the liquid and the vapor phase. For zeotropes, the heat transfer performance will be less than a linear interpolation between the pure components (Thome 1990). One of the more common approaches for predicting zeotropic mixture boiling is to model the heat transfer degradation rather than the absolute value of the heat transfer performance.

There are two fundamental thermodynamic differences between single-component fluids and mixtures which, in turn, cause fundamental differences between their phase change characteristics. First, at constant pressure, the mixture temperature rises during evaporation, while the temperature of the single-component fluids remains constant. Second, the liquid and vapor compositions are different in the mixture, while they are identical in the single component. These points are demonstrated by the phase equilibrium diagrams shown in Fig. 1 for a hypothetical mixture of a more volatile fluid and a less volatile fluid.

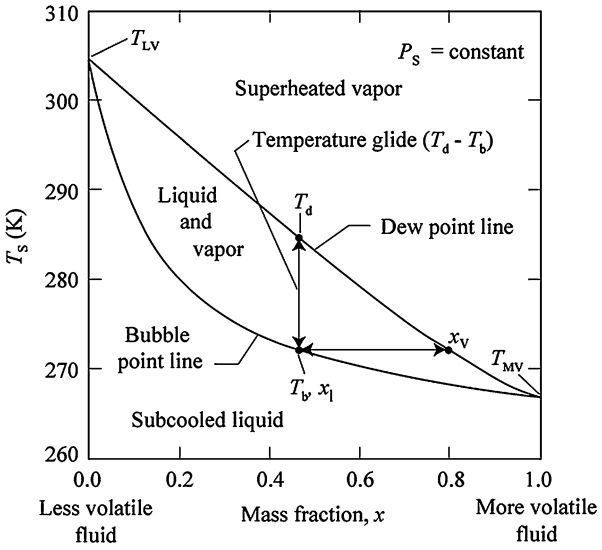

Fig. 1 Example phase equilibrium diagram at fixed pressure

Figure 1 shows the phase equilibrium diagram for a binary mixture at a fixed saturation pressure (P_s) with the saturation temperature (T_s) plotted on the ordinate and the mass composition (x) on the abscissa. Figure 1 represents the thermodynamic state of the mixture at equilibrium conditions. The more volatile (MV) component is identified by a saturation temperature that is lower than that of the less volatile (LV) component at the same pressure. The lower line, the bubble point line, represents the variation of the liquid saturation temperature with composition. The bubble point line identifies the transition between all-liquid to the initiation of vapor. The upper line, the dew point line, represents the variation of the saturated vapor temperature with composition and the transition from all-vapor to the initiation of condensation. The area between the dew point and bubble point lines represents a two-phase mixture with a liquid of composition x_l and a vapor of composition x_v in coexistence. The vertical distance between the dew point and bubble point lines is called the temperature glide. As a general rule of thumb, the fraction of the length of the vertical line between the dew point and the bubble point lines is approximately equal to the thermodynamic quality of the mixture. For example, the midpoint between T_d and T_b approximately corresponds to a quality of 50%. Similarly, 20% up from T_b approximately corresponds to a 20% quality. Depending on the mixture interaction parameter, this approximate relationship can be less accurate for mixed components with large differences in normal boiling point.

A horizontal line connecting the bubble point and the dew point lines gives the composition of the liquid and the composition of the vapor at the point where it contacts the bubble point line and the dew point line, respectively. The same is true for a horizontal line intersecting the temperature glide at a quality of 50%, corresponding to the liquid and vapor composition at that quality. The temperature glide may loosely be used to determine the potential for differences between x_l and

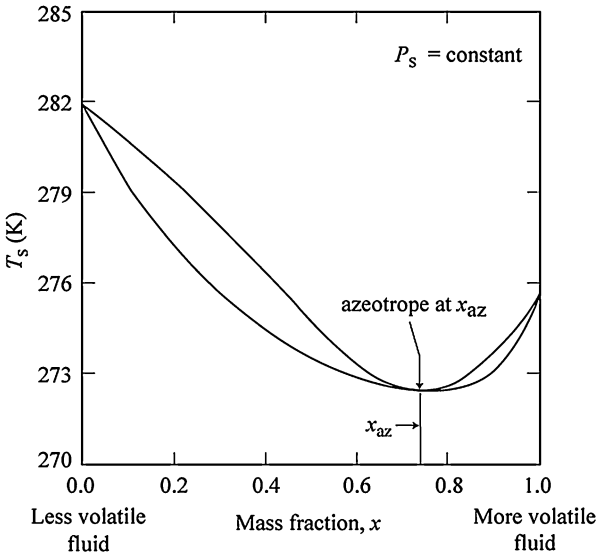

Fig. 2 Phase equilibrium diagram for azeotrope at constant pressure

x_v. Larger glides imply larger $x_v - x_l$ and corresponding larger heat transfer degradations. Part of the degradation is caused by what Shock (1982) has termed the `loss of available superheat`. This loss is a consequence of the mixture equilibrium temperature approaching the temperature of the heated wall as it becomes higher quality two-phase, thus reducing the driving temperature difference. Further discussion of mixture phase equilibrium can be found in Shock (1982).

Figure 1 represents the behavior of a binary zeotropic mixture. An azeotrope, which is a mixture that has no temperature glide at a particular composition, is likely to exhibit very little heat transfer degradation. Figure 2 shows that an azeotrope exists at x_{az} as depicted by the intersection of the dew and bubble lines.

2.1 Thermodynamic Properties

Thermodynamic properties are predicted by an equation of state (EOS) because measurements are seldom sufficient to cover all desired conditions, and because many thermodynamic properties are derived properties. A particular EOS is developed by using the existing fluid equilibrium measurements for single-component fluids and fitting the constants of the EOS. Typically, interaction parameters are then fitted to mixture data in order to enable the EOS to predict the thermodynamic properties of mixtures. Some EOSs are specific to a type of fluid. For example, the National Institute of Standards and Technology (NIST) Standard Reference Data software REFPROP (Lemmon et al. 2013) was originally designed to predict the properties of refrigerants and binary-refrigerant mixtures. The current version of REFPROP has the capability of predicting multicomponent mixtures of many other industrial fluids that are not typically refrigerants.

2.2 Transport Properties

Access to an EOS program generally will provide all the necessary transport properties of volatile mixtures. However, if transport properties are not available for mixtures, a first approximation for the prediction of thermal conductivity, specific volume, and surface tension can be obtained from linear ($f = 1$), mass- or mole-fraction-weighted property (Y_m) as a summation of the pure component properties, Y_i (Reid et al. 1977):

$$Y_m^f = \sum_i^n x_i Y_i^f \tag{1}$$

Here, Y_m is the mixture property and Y_i is the property of the ith component of the mixture of n components. The x_i is either the mass fraction of ith component in the mixture or the mole fraction of ith component depending on whether Y_i is a mass-based or a mole-based property, respectively. Equation (1) will fail to adequately predict mixtures of fluids with widely different normal boiling points and/or chemically dissimilar fluids. For these cases, the prediction can be improved by using mixture specific values for the exponent f. Note that the specific volume is the reciprocal of the density and that Eq. (1) is not valid for density unless the volume fraction is used instead of the mass or mole fraction. Properties may require a property-specific mixing model. A few of these models are given below.

2.2.1 Viscosity Predictions

Reid et al. (1977) provide a mixture model for the kinematic viscosity (ν) of liquid, which is a mass-fraction-weighted sum of the natural log of the component kinematic viscosities:

$$\ln \nu_m = \sum_i^n x_i \ln \nu_i \tag{2}$$

Equation (2) is valid for mole-based viscosities if the mole fraction is used in place of the mass fraction.

2.3 Nanofluid Properties

2.3.1 Nanofluid Viscosity

For nanolubricants, Kedzierski (2013) developed a model, as shown in Eqs. (3) through (5) below, based on a modified version of the above mass-fraction-weighted method. The viscosity model is the mass-fraction-weighted sum of the natural log of the component kinematic viscosities of the nanoparticle, the surfactant, and the base liquid lubricant:

$$\ln \nu_m = x_L^{1.25} \ln \nu_L + x_{\text{np}}^{1.25} \ln \nu_{\text{np}} + x_s^{1.25} \ln \nu_s \tag{3}$$

Equation (3) is nearly the same as the equation recommended by Reid et al. (1977) with the exception that the exponents on the mass fractions for Reid et al. (1977) are 1 rather than 1.25. For Eq. (3), ν_m is the liquid kinematic viscosity, ν_L is the kinematic viscosity of the base liquid, ν_s is the kinematic viscosity of the surfactant, and ν_{np} is the pseudo-kinematic viscosity of nanoparticle given as:

$$\ln \nu_s = 0.149 D_p[\text{nm}] - 87.2079 + \frac{7.1353}{T_r^{-66.12} + 0.074} \tag{4}$$

$$\ln \nu_{\text{np}} = \left(1.426 - 0.0071 D_p[\text{nm}]\right)\left(4.7356 + \frac{1.4706}{T_{\text{r}}^{4.05} - 1.11}\right) \tag{5}$$

where the kinematic viscosity has units of $\text{mm}^2 \cdot \text{s}^{-1}$, and the diameter of the nanoparticle (D_p) has units of nm. T_r is the dimensionless liquid temperature normalized by 273.15 K, i.e., $T_r = T/273.15$ K. T is the temperature of the liquid in Kelvin.

The model assumes that a good dispersion exists whereby the surfactant is more closely associated with the nanoparticle than it is with the base liquid (i.e., lubricant). Equations (4) and (5) do not represent the viscosities of the pure surfactant and the nanoparticles, respectively. Rather, as evidenced by the D_p term, they are pseudo-viscosities that each account for the interaction between the nanoparticle and the surfactant. The model was developed for a specific surfactant using nanolubricant viscosity measurements. Prediction errors associated with nanolubricants with surfactants of differing viscosity may be significant if the surfactant mass fractions are greater than 6% (Kedzierski et al. 2016).

2.3.2 Nanofluid Density

The liquid mixture density (ρ_m) should be calculated from a linear mass-fraction (x) weighted sum of the single component values of the specific volumes (ρ_m^{-1}) for a given temperature (T) (Reid et al. 1977):

$$\frac{1}{\rho_m} = \frac{x_{\text{s}}}{\rho_s} + \frac{x_L}{\rho_L} + \frac{x_{\text{np}}}{\rho_{\text{np}}} \tag{6}$$

The above equation may also be used to calculate the density of a nanofluid that includes the base fluid (ρ_L), surfactant (ρ_s), and the nanoparticles (ρ_{np}).

2.3.3 Nanofluid Thermal Conductivity

For nanofluid thermal conductivities (k_n), the heterogeneous media model for spherical and well-dispersed particles that is attributed to Maxwell (1954) is:

$$k_n = \frac{k_{\mathrm{np}} + 2k_L + 2\phi\left(k_{\mathrm{np}} - k_L\right)}{k_{\mathrm{np}} + 2k_L - \phi\left(k_{\mathrm{np}} - k_L\right)} k_L \tag{7}$$

where the thermal conductivity of the nanoparticle (k_{np}), the thermal conductivity of the pure (i.e., base) lubricant (k_L), and the volume fraction of the nanoparticles in the nanolubricant (ϕ) are inputs to Eq. (7). The actual equation that Maxwell (1954) developed was for electrical resistivity rather than thermal conductivity. Somewhere along the way, someone used the Wiedemann–Franz law (Tipler 1978) to translate Maxwell's development to Eq. (7). Because of this, a further restriction on Eq. (7), beyond spherical particles, is how well the thermal conductivities of both the base fluid and the nanoparticle remain linearly related to their electrical resistivities as dictated by the Wiedemann–Franz law (Tipler 1978). One could imagine that if the relationship between resistivity and thermal conductivity varies in the same nonlinear way for the nanoparticle as it does for the base fluid that this effect would cancel and Eq. (7) would still be valid for this case.

Bigi et al. (2015) reported that the thermal conductivity of nanolubricants was predicted well with Eq. (7) for spherical 40 nm diameter γ-Al_2O_3 nanoparticles. They also showed that γ-Al_2O_3 nanoparticles, at a 20% mass fraction, can increase the thermal conductivity of lubricants by 10 and 40% for temperatures of 5 °C and 40 °C, respectively.

Surfactants play a critical role in preventing agglomeration and sedimentation of the nanoparticles dispersed in the base lubricant. Cremaschi et al. (2015) measured the agglomeration of nanoparticles in presence of three distinct surfactants that had decreasing degree of polarity; and one surfactant was effective in preventing agglomeration and sedimentation of the nanoparticles in the refrigerant and lubricant mixture. Cremaschi et al. (2014) showed that surfactants can influence nanolubricant thermal conductivity by as much as ±7.2%. The effect of surfactants can be predicted by using a mixture value for the surfactant/lubricant in Eq. (7) for k_{L}.

For nonspherical nanoparticles, Hamilton and Crosser (1962) modified Maxwell's equation with the sphericity (Ψ):

$$k_{\mathrm{nL}} = \frac{k_{\mathrm{np}} + \left(\frac{3}{\Psi} - 1\right)k_L + \left(\frac{3}{\Psi} - 1\right)\phi\left(k_{\mathrm{np}} - k_L\right)}{k_{\mathrm{np}} + \left(\frac{3}{\Psi} - 1\right)k_L - \phi\left(k_{\mathrm{np}} - k_L\right)} k_L \tag{8}$$

The sphericity is defined as the ratio of the surface area of a particle-volume-equivalent sphere to the actual surface area of the particle (Clift et al. 1979), which is less than one for particles that are not spherical.

Kedzierski et al. (2016) and Deokar et al. (2016) provide thermal conductivity measurements for ZnO-based nanolubricants. The ZnO nanoparticles are nonspherical nanoparticles, having an elongated hexagonal wurtzite-like shape, and a corresponding sphericity of approximately 0.55.

3 Composition Gradients

Gradients in the composition of the liquid are an important part of modeling mixture boiling because the composition determines the local equilibrium temperature of the liquid film, which, in turn, governs the heat transfer (Schluender 1983). Composition gradients can exist over rather short distances within a narrow diffusion boundary layer region at the liquid–vapor interface where evaporation occurs or over larger distances between thick and thin regions of a liquid film (Kedzierski et al. 1992). For film thickness approaching the thickness of the diffusion boundary layer, variation in the film thickness may cause variation in the composition because evaporation may affect to bulk composition of the liquid film as explained below.

Figure 3 shows an evaporating liquid film on a heated wall where the liquid of a binary mixture changes to vapor at the liquid–vapor interface. Fig. 3 illustrates the composition gradients in x that are established within a liquid binary-mixture film, at two different y-locations, as a consequence of preferential evaporation of the more volatile component. Evaporation occurs at the liquid–vapor interface, which depletes that region of the more volatile component resulting in a layer that is of a composition that is more concentrated in the less volatile component than the bulk fluid. As

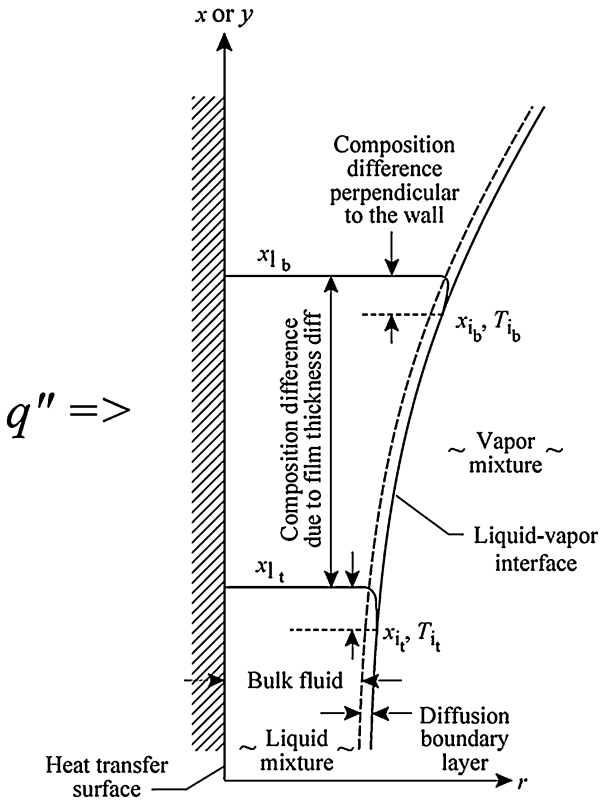

Fig. 3 Composition gradients within the liquid film

shown in Fig. 3, the composition gradient is confined to a narrow region called the diffusion boundary layer. The more volatile component diffuses from the bulk liquid to the liquid–vapor interface while the less volatile component diffuses from the liquid–vapor interface to the bulk liquid. Larger rates of evaporation cause greater depletion of the more volatile component because of the relatively fixed net-mass in the liquid–vapor interface. The evaporation rate and the diffusion interact to determine the size of the composition gradient and the resulting liquid–vapor interface composition (x_i). For a given boiling surface temperature (T_w), the x_i determines the driving temperature difference by setting the saturation temperature at the interface (T_s). An equation that relates diffusion to local composition is typically used to determine x_i (Schluender 1983).

Composition gradients in mixtures have also been observed to occur within the bulk liquid film due to varying film thickness (Jung et al. 1989). If the liquid film is thin enough that evaporation at the liquid–vapor interface reduces the bulk composition of the more volatile component, the composition can vary with film thickness. Figure 3 shows the mass fraction coordinate along the wall and increasing in the vertical y-direction. The mass fraction of the more volatile component in the thin-film (x_{lt}) region is less than that of the thick-film (x_{lb}) region because the thin-film region, having less mass but nearly the same heat input, is depleted of the more volatile component, which results in a shift in composition toward the least volatile component. Consequently, a film thickness gradient has induced a composition gradient along the heated surface by having varying degrees of depletion of the more volatile component due to differences in liquid mass.

One obvious mixture phase change phenomenon exhibiting film thickness variations as shown in Fig. 3 is an evaporating falling film. Another application of Fig. 3 is for annular flow boiling in a horizontal tube. Because gravity imposes a non-uniform circumferential film thickness distribution for horizontal annular flow, circumferential composition gradients can exist. Circumferential composition gradients cause the temperature of the liquid–vapor interface at the top of the tube (T_{it}) to be greater than that at the bottom of the tube (T_{ib}). The magnitude of the liquid–vapor interface temperature is determined by both the circumferential and the radial composition gradients.

The composition gradient perpendicular to the heated surface exists primarily within the thickness of the diffusion boundary layer at the liquid–vapor interface, as shown in Fig. 3. Turbulent mixing prevents the formation of composition gradients within the bulk liquid (Kedzierski et al. 1992). In summary, evaporation depletes the diffusion boundary layer of the more volatile component and the convection confines the composition gradient to a narrow region within or close to the liquid–vapor interface.

4 Pool Boiling of Mixtures

Cooper (1984) provides a simple, albeit dimensionally corrupt, model for the nucleate pool boiling heat transfer coefficient (h_{nb}) for single-component and azeotropic fluids on a flat horizontal surface:

$$h_{\mathrm{nb}} = 55\left(\frac{P_s}{P_c}\right)^{0.12-0.2\log_{10}R_p}\left(-\log_{10}\frac{P_s}{P_c}\right)^{-0.55} M_w^{-0.5}\left(q''\right)^{0.67} \tag{9}$$

The units are g per mole, W m^{-2} K, W m^{-2}, and μm for M_w, h_{nb}, q'', and R_p, respectively. Here, R_p is the average roughness of the boiling surface. P_s is the local equilibrium pressure and P_c is the critical pressure of the mixture.

Thome (1989) modified a model proposed by Schluender (1983) in order to make Cooper's equation valid for the pool boiling heat transfer of multicomponent mixtures (h_{mb}):

$$h_{\mathrm{mb}} = h_{nb}\left\{1 + \frac{h_{nb}}{q''}\left(T_d - T_b\right)\left[1 - \exp\left(\frac{-q''}{\rho_m h_{fg} i_m}\right)\right]\right\}^{-1} \tag{10}$$

where h_{nb} in Eq. (10) is obtained from Eq. (9) evaluated at the mixture properties. Here h_{fg} is the latent heat of vaporization of the mixture and i_m is the mass transfer coefficient, which is a constant value of 0.0003 m s^{-1}.

5 Prediction of Mixture Flow Boiling in Horizontal Smooth Tubes

The Zou et al. (2010) correlation for binary mixture flow boiling in a smooth tube is based on a superposition of a single-phase convection heat transfer coefficient (h_c) and a nucleate boiling heat transfer coefficient (h_{nb}):

$$h_{\mathrm{mb}} = \sqrt{\left(Eh_c\right)^2 + \left(\frac{Sh_{\mathrm{nb}}}{K}\right)^2} \tag{11}$$

The correlation follows the path of the pioneering work of Chen (1966), where a Reynolds number enhancement factor (E) along with a nucleate boiling suppression factor (S) are used as modifiers for component heat transfer coefficients. The K factor in Eq. (11) is used to model the mixture heat transfer effects. The suppression factor models the effect of the waning of the h_{nb} component as the flow quality increases. The h_{nb} is calculated from Cooper's correlation (1984) given in Eq. (9). The heat transfer coefficient for single-phase convection (h_{c}) is calculated from the Dittus–Boelter equation (Incropera and DeWitt 2002):

$$h_c = 0.023\mathrm{Re}^{0.8}\mathrm{Pr}^{0.4}\frac{k_l}{D_i} \tag{12}$$

Here, Re and Pr are the all-liquid Reynolds and Prandtl numbers, respectively, evaluated as if the entire flow was liquid. The k_l is the liquid thermal conductivity and D_i is the inner diameter of the smooth tube.

The enhancement factor (E) accounts for the fact that momentum transfer for a two-phase flow will be greater than that of a single-phase flow due to the larger pressure drop and is calculated as:

$$E = \left[1 + x_q\mathrm{Pr}\left(\frac{\rho_l}{\rho_v} - 1\right)\right]^{0.35} \tag{13}$$

Here, x_q is the local thermodynamic quality and Pr is the all-liquid Prandtl number.

The suppression factor (S) is calculated from:

$$S = \left[1 + 0.055E^{0.1}\mathrm{Re}^{0.16}\right]^{-1} \tag{14}$$

Here, the Re is the all-liquid Reynolds number and E is calculated from Eq. (13).

The Zou et al. (2010) correlation uses the K factor, which is unfortunately dimensional, to account for mixture heat transfer effects:

$$K = 1 + \frac{(T_d - T_b)h_i}{q''}|x_{\mathrm{mv}} - x_{\mathrm{ml}}|^{-0.29}\left(\frac{P_s}{10^5}\right)^{-0.9}\left[1 - 0.87\exp\left(\frac{-q''}{3\times 10^5}\right)\right] \tag{15}$$

where the units of q'', h_i, and P_s are kW m^{-2}, kW m^{-2} K^{-1}, and kPa, respectively. Here, x_{mv} and x_{ml} are the mole fractions of the vapor and the liquid evaluated at the local quality, respectively. The ideal binary mixture heat transfer coefficient (h_i) is obtained from a linear mole-fraction-weighted average of the single-component heat transfer coefficients, each evaluated from Eq. (9), of the more volatile and the less volatile components: $h_i = h_{\mathrm{MV}}h_{\mathrm{LV}}/((1 - x_{\mathrm{ml}})h_{\mathrm{MV}} + x_{\mathrm{ml}}h_{\mathrm{LV}})$. A first approximation for extending the Zou et al. (2010) binary mixture model to multicomponent mixtures would be to use $h_{\mathrm{nb,}}$ evaluated from Eq. (9) at the overall composition, in place of h_i. In addition, it is recommended to use the largest difference between the vapor and the liquid composition when evaluating $|x_{\mathrm{mv}} - x_{\mathrm{ml}}|$ for multicomponent mixtures.

6 Prediction of Flow Boiling in Horizontal Micofin Tubes

Thome (1999) provides a good review of flow boiling correlations for flow boiling in microfin tubes. The Hamilton et al. (2008) correlation is presented here for its simplicity and generalized geometric base for predicting local convective boiling

Nusselt numbers (Nu). The single-component version of the Hamilton et al. (2008) correlation valid for azeotropic refrigerants is:

$$Nu_p = \frac{hD_h}{k_l} = 482.18\mathrm{Re}^{0.3}\mathrm{Pr}^{C_1}\left(\frac{P_s}{P_c}\right)^{C_2} Bo^{C_3}\left(-\log_{10}\frac{P_s}{P_c}\right)^{C_4} {M_w}^{C_5} \tag{16}$$

where

$$C_1 = 0.51x_q$$

$$C_2 = 5.57x_q - 5.21x_q^2$$

$$C_3 = 0.54 - 1.56x_q + 1.42x_q^2$$

$$C_4 = -0.81 + 12.56x_q - 11.00x_q^2$$

$$C_5 = 0.25 - 0.035x_q^2$$

Here, the all-liquid Reynolds number (Re), the boiling number (Bo), the all-liquid Prandtl number (Pr), the reduced pressure (P_s/P_c), and the quality (x_q) are all evaluated locally at the saturation temperature. All-liquid dimensionless parameters are used because the variation of Nu_p with quality is provided by the quality-dependent exponents, C_1 through C_5. The all-liquid Reynolds number and the Nusselt number are based on the hydraulic diameter (D_h). The M_w is the molecular mass that must have units of g per mole. Most correlations in the literature are based on the projected-smooth area of the microfin tube. For the above correlation, the Boiling number, the Nusselt number, the heat flux ($q'' = q/A_i$), and the heat transfer coefficient ($h = q/(A_i(T_w - T_s))$) are based on the actual inner surface area per unit length (A_i/L) of the tube, which can be estimated for a microfin tube from:

$$\frac{A_i}{L} = N_f\left(\frac{s}{\cos\alpha} + \frac{2e}{\cos\alpha\cos(\beta/2)}\right) \tag{17}$$

where s is the spacing between the fins, β is the fin-tip angle, e is the fin height, α is the twist angle of the fins, t_b is the thickness of the fin at its base, N_f is the total number of fins, and D_r is the diameter of the tube at the fin root as shown in Fig. 4.

The hydraulic diameter (D_h) of the microfin tube can be estimated from (Kedzierski and Goncalves 1999):

$$D_h = \frac{4A_c\cos\alpha}{N_f S_p} = \frac{\left(\pi D_r^2 - 2N_f t_b e\right)\cos\alpha}{s + \dfrac{2e}{\cos(\beta/2)}} \tag{18}$$

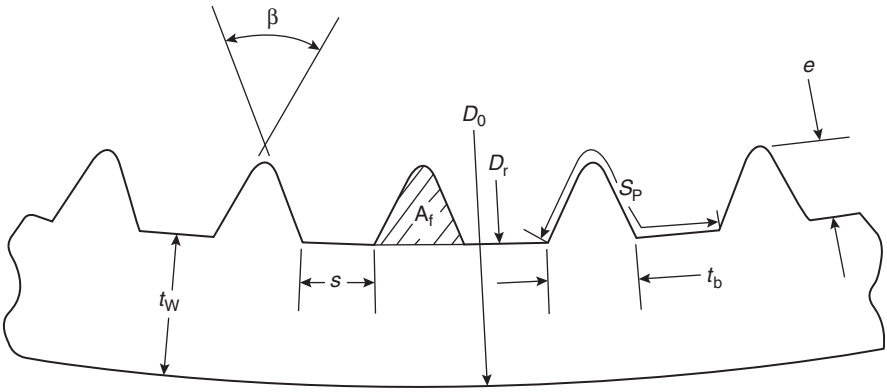

Fig. 4 Detailed cross section of typical microfin tube

The fin parameters that are used in Eqs. (17) and (18), where S_p is the perimeter of one fin and channel taken perpendicular to the axis of the fin, and A_c is the cross-sectional flow area, $A_c = \frac{\pi D_o^2}{4} - N_f A_f$, as shown in Fig. 4.

Hamilton et al. (2008) also provide a correction factor for Eq. (16) to predict the heat transfer coefficient for binary mixtures, which cannot be used for mixtures of more than two components. Consequently, Kedzierski and Kang (2016) developed a new correction for Eq. (16) to predict the flow boiling Nusselt number (Nu) for mixtures of any number of refrigerants. This was done by multiplying the single-component Nusselt number (Nu_p) by a modifier to predict multicomponent mixtures (Nu_m):

$$Nu_m = Nu_p\left(1 - 36.23\left[\frac{T_d - T_b}{T_b}\right]\exp\left(-0.007\mathrm{Re}Bo^{0.47}\right)\right) \tag{19}$$

where T_d and T_b are the dew point and bubble point temperatures (Fig. 1), respectively, evaluated at the local saturation pressure and overall composition of the mixture. Typically, large temperature glides cause composition gradients that lead to heat transfer degradations as compared to what would be expected from a single-component prediction model (Kedzierski et al. 1992). Consequently, the parenthetical term in Eq. (19) that multiplies Nu_p describes the mixture degradation effect, which is a function of temperature glide, Bo and Re. A single-component refrigerant would have zero temperature glide, which would result in the mixture degradation effect, represented by the parenthetical term, being equal to one.

7 Refrigerant/Lubricant Mixture Boiling

In many applications, refrigeration and air-conditioning equipment require compressor lubricating oil for the safe operation of the compressor. The lubricant is practically impossible to confine to the compressor and makes its way to the evaporator and forms a dilute mixture with the refrigerant. Being that the vapor pressure is very low, the lubricant does not evaporate and remains in liquid form. Because of its relative nonvolatility, the composition of the lubricant in the liquid increases in an evaporating refrigerant/lubricant mixture flowing inside a tube. For a pool boiling surface, a lubricant excess layer, which is nearly all lubricant, forms at a thickness of approximately 40 microns at the boiling surface (Kedzierski 2002). The term excess expresses that the lubricant composition at the boiling surface is in excess of the composition in the bulk liquid. The presence of the lubricant in the bulk liquid and the excess layer influences the transport properties and, to a smaller degree, the vapor pressure equilibrium of the refrigerant.

For in-tube convective flow boiling, the presence of lubricant tends to promote early formation of annular flow (Radermacher et al. 2006). Lubricant mixed with refrigerant causes a decrease in refrigerant heat transfer because the lubricant induces an increase in the liquid viscosity and changes the equilibrium pressure, which effectively reduces the superheat. However, when the mass fraction of the lubricant is less than 1%, the effect of the lubricant on the evaporation heat transfer rate is generally small. Two-phase flow pressure drops in tubes can increase significantly when lubricant is present due to the increase in the viscosity of the liquid on the tube wall (Cremaschi et al. 2005, 2016; Choi et al. 2001).

7.1 Nucleate Boiling of Refrigerant/Lubricant Mixtures

In order to model the pool boiling of refrigerant/lubricant mixtures, knowledge of the lubricant film, called the lubricant excess surface density (Γ), must be obtained. The addition of lubricant to pure refrigerant changes the boiling behavior in two ways. Because of the presence of the lubricant excess layer, the Gibbs adsorption equation dictates that a reduction in surface energy between the boiling surface and the fluid must exist (Kedzierski 2001). The reduced surface energy causes a reduction in the forces that hold the bubble to the boiling surface. Consequently, the bubble does not have to grow very large before buoyancy forces are sufficient to remove the bubble from the surface, resulting in reduced bubble size. Smaller bubbles can now grow to completion within the thermal boundary layer. Larger bubbles would not exist, because they would grow beyond the thermal boundary layer and recondense. Thus, the second difference is that lubricant induces an increase in the bubble site density.

Figure 5 outlines the Kedzierski (2003a) model for refrigerant/lubricant pool boiling. Bubbles are shown growing through lubricant excess layers of three different thicknesses (l_e). The thickness l_e is determined from a balance between lubricant deposited to the layer as the refrigerant evaporates and lubricant removed by the departing bubbles. As the bubble departs, it removes a thickness of the lubricant

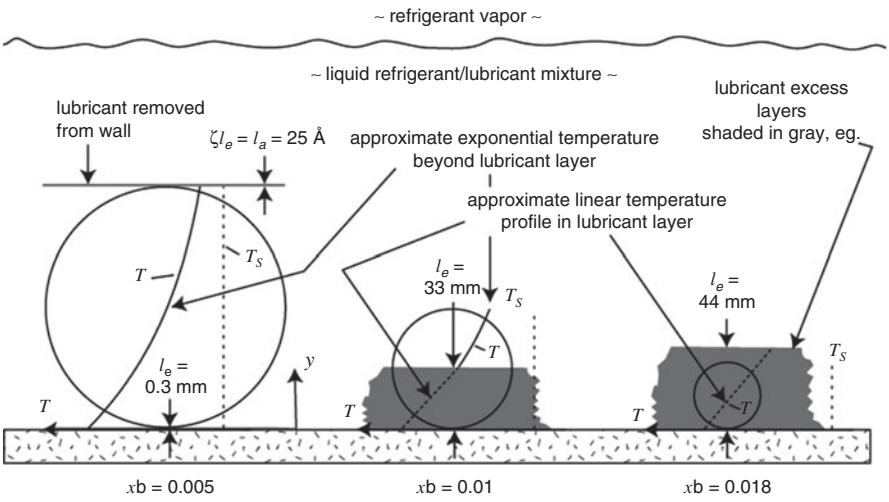

Fig. 5 Schematic of the average departure bubble for three R123/lubricant mixtures with corresponding excess layers (Kedzierski 2001)

dictated by that which Van der Waals forces may hold to the bubble, which is approximately 25 Å for lubricants (Laesecke 2002). Using the above assumptions, an expression for the departure bubble radius (r_b) for refrigerant/lubricant mixtures can be written based on a lubricant mass balance (Kedzierski 2003a):

$$r_b = \frac{0.75\zeta l_e \rho_L (1 - x_b)}{x_b \rho_{rv}} = \frac{18.75\text{Å}\rho_L (1 - x_b)}{x_b \rho_{rv}} \tag{20}$$

where x_b is the mass fraction of the lubricant in the bulk mixture, ρ_L is the mass density of the lubricant, ρ_{rv} is the mass density of the refrigerant vapor, and 25 Å was substituted for ζl_e per the preceding discussion. Eq. (20) is valid for $x_b > 0$.

The excess surface density (Γ) is the mass of lubricant per unit surface area that is confined to the excess layer (l_e) at the wall. The excess layer is essentially all lubricant. The term excess is used because the mass fraction of lubricant within l_e is in excess of the lubricant mass fraction of the bulk liquid. The nondimensional constant that was derived from excess surface density (Γ) measurements in Kedzierski (2003b) was given as:

$$\frac{x_b T_s \sigma (\rho_L - \rho_b x_b)}{\Gamma (1 - x_b) \rho_L h_{fg} \Delta T_s} = 5.9 \times 10^{-7} \tag{21}$$

where σ is the refrigerant liquid–vapor surface tension, h_{fg} is the latent heat of the refrigerant, T_s is the saturation temperature of the refrigerant, ρ_b is the liquid density of the bulk refrigerant/lubricant mixture, and ΔT_s is the wall superheat.

Equation (21) can be solved for l_e by using an approximate definition of the excess surface density, $\Gamma = l_e(\rho_L - \rho_b x_b)$:

$$l_e = \frac{\Gamma}{\rho_L - \rho_b x_b} = \frac{x_b T_s \sigma}{5.9 \times 10^{-7}(1 - x_b)\rho_L h_{fg} \Delta T_s} \tag{22}$$

The value of l_e is important because the temperature profile is assumed to be linear within the lubricant excess layer. Beyond the excess layer, the thermal boundary layer is assumed to decay exponentially to the saturation temperature of the bulk fluid (T_s). The thermal boundary layer parameter, λ, determines the rate of decay of the fluid temperature. Kedzierski (2003b) gave λ, which is valid for $0 < \lambda l_e / r_b < 2.5$, as:

$$\lambda = \frac{r_b \Gamma^2 h_{fg} / l_e}{\dfrac{k_L \Delta T_s (\rho_L - \rho_b x_b) x_b}{A_0 e^{b\Delta T_s}(1 - x_b)} - 0.62\Gamma^2 h_{fg}} \tag{23}$$

Finally, the refrigerant/lubricant heat transfer coefficient (h_{pL}) valid for $x_b > 0$ was given as:

$$h_{\mathrm{pL}} = \frac{q''_{\mathrm{pL}}}{T_w - T_s} = \frac{5.9 \times 10^{-7}(1 - x_b)\rho_L h_{fg} \Delta T_s k_L \left(1 - e^{-\lambda l_e / r_b}\right)}{x_b T_s \sigma} \tag{24}$$

where Eqs. (20), (22), and (23) are used to calculate r_b, l_e, and λ, respectively. The subscript "pL" represents the refrigerant and "plain" lubricant mixture in order to differentiate it from refrigerant/nanolubricants, which are discussed in Section 8.2.

7.2 Convective Boiling of Refrigerant/Lubricant Mixtures

Convective boiling of a volatile fluid, like a refrigerant, is affected by the addition of lubricant primarily because lubricant significantly increases the viscosity of the mixture and changes the equilibrium vapor pressure. These effects strengthen as the local lubricant mass fraction (w_l) increases as the flow quality (x_q) increases:

$$w_l = \frac{w_b}{1 - x_q} \tag{25}$$

Here, w_b is the bulk lubricant mass fraction for the all-liquid condition at zero quality.

Thome (1995) outlines a methodology for predicting the saturated temperature–pressure relationship for a refrigerant/lubricant mixture:

$$\frac{1}{T_r} = \frac{\ln(P_r) - b + \dfrac{A_2}{A_1} x_q}{c} \tag{26}$$

Thome (1995) provides c and b as fourth-degree polynomials in the local lubricant mass fraction in the refrigerant liquid (w_l):

$$c = -2300.2[\mathrm{K}] + 182.5[\mathrm{K}]w_l - 724.2[\mathrm{K}]w_l^2 + 3868.0[\mathrm{K}]w_l^3 - 5268.9[\mathrm{K}]w_l^4$$
$$b = 15.146 - 0.722w_l + 2.391w_l^2 - 13.779w_l^3 + 17.066w_l^4 \tag{27}$$

All of the coefficients of the c (units of K) and b polynomials with the exception of the constant terms were taken from Thome (1995). The constant terms of the polynomials were adjusted by Sawant et al. (2007) to the lubricant-free R410A expression given in Eq. (26) when $w_l = 0$.

Choi et al. (2001) found that the two-phase pressure drop of refrigerant/lubricant mixtures could be predicted acceptably well with standard correlations using the local refrigerant/lubricant mixture viscosity in the calculation of the Reynolds number and pure-refrigerant properties elsewhere. Considering this, Sawant et al. (2007) showed, and Bigi and Cremaschi (2016) verified, that refrigerant/lubricant convective boiling in a microfin tube could be predicted to with ±20% by using the Hamilton et al. (2008) correlation (Eq. (16)) with the refrigerant/lubricant mixture liquid viscosity and liquid density evaluated at the local lubricant mass fraction to calculate Re and Pr for use in Eq. (16). Use of the lubricant properties in the correlation caused between a 0.3% and a 0.8% reduction in the Nusselt number as compared to results using the lubricant-free R410A properties alone. Being that Sawant et al. (2007) showed that for qualities less than 50%, the lubricant changed the saturation temperature of R410A by less than 0.022 K; neglecting the effect on pressure may yield acceptable results. It is expected that a fair prediction for convective refrigerant/lubricant boiling in *smooth* tubes may be achieved by using the local mixture viscosity in the calculation of Re and Pr in the Zou et al. (2010) model, i.e., Eqs. (11)–(15).

For smooth tubes, Chaddock and Mathur (1980) propose that refrigerant/lubricant flow boiling when nucleate boiling is fully suppressed be correlated in the form:

$$h = h_c C \left(\frac{1}{\chi_{\mathrm{tt}}}\right)^n \tag{28}$$

where C and n are paired correlating constants for a particular refrigerant/lubricant mixture and lubricant concentration. The Lockhart–Martinelli parameter (χ_{tt}) varies with quality, x_q, consists of liquid and vapor fluid properties, and is given in the Nomenclature. For the χ_{tt} in Eq. (28), the vapor density and the vapor dynamic viscosity are evaluated as pure refrigerant vapor. In addition, the liquid density, the liquid dynamic viscosity, and the quality are evaluated as mixed refrigerant/lubricant properties at the lubricant mass fraction. When evaluating Eq. (12) for use in Eq. (28), only the dynamic viscosity is evaluated as a refrigerant/lubricant mixture. All other properties in Eq. (12) are taken as pure liquid-refrigerant values. Table 1 provides values for C and n, as taken from Chaddock and Mathur (1980), for various

Table 1 Chaddock and Mathur (1980) refrigerant/lubricant flow boiling constants for Eq. (28)

Mass % oil in R22	C	n	% of data fitted to within ±35%
0	3.90	0.62	93
1.0	4.72	0.59	95
2.9	4.36	0.60	88
5.7	4.97	0.59	89

percent mass fractions of a naphthenic oil, with a nominal kinematic viscosity of 21.58×10^{-6} m^2 s^{-1} at 100 °C, in R22.

In addition to the above discussed lubricant effects, Thome (1995) discusses the influence of the specific heat of the lubricant on the enthalpy change of the refrigerant/lubricant mixture and provides a methodology for its calculation. The effect of lubricant-specific heat on refrigerant/lubricant flow boiling becomes more significant for larger lubricant concentrations and larger thermodynamic qualities. The lubricant transports heat that is not used to evaporate refrigerant. Consequently, the heat capacity of the lubricant is a source of loss of available energy for phase change, which leads to a degradation in heat transfer.

8 Nanofluids Pool Boiling

8.1 Water-Based Nanofluid Boiling

The boiling data with water-based nanofluids is inconsistent. Some measurements show enhancement with respect to pure water and others show boiling degradations (Barber et al. 2011). The reason for this is that due to the relatively low viscosity of water, it is difficult to have a stable nanofluid that does not exhibit settling. Settling of nanoparticles onto the boiling service has the potential to fill active cavity sites on the surface, thus reducing the boiling performance. Nanofluid stability can be improved with a surfactant, but the surfactant may contribute to boiling enhancement by reducing the surface tension of water. Consequently, successful, generalized modeling of water-based nanofluids has not been accomplished, which makes reliable prediction of water-based nanofluids difficult (see ▶ Boiling with Nano Particles).

8.2 Prediction of Refrigerant/Nanolubricant Pool Boiling

Because of the heat transfer degradation caused by the addition of lubricant to refrigerant, enhancement techniques for refrigerant/lubricant boiling are of high interest. A cost-effective way of enhancing the boiling performance of refrigerant/lubricant mixtures is to add nanoparticles to the lubricant. For example, Kedzierski and Gong (2009) have shown that copper-oxide nanoparticles can increase the refrigerant/lubricant pool boiling heat flux by as much as 245%, and Kedzierski

(2011, 2012) has shown that aluminum-oxide nanoparticles can yield similar enhancements for refrigerant/lubricant pool boiling.

The existence of the lubricant excess layer provides an opportunity for heat transfer enhancement by providing an environment where the nanoparticles can be in stable Brownian motion. Nanofluid boiling with less viscous base fluids, like water, typically results in the cavities of the boiling surface being filled with trapped nanoparticles resulting in a heat transfer degradation. The lubricant excess layer prevents nanoparticle settling and allows the nanoparticles to be suspended above the surface.

Equation 29 gives the pool boiling heat flux for a refrigerant/nanolubricant mixture (q''_{np}) normalized by the pool boiling heat flux for a refrigerant/lubricant mixture (q''_{PL}) of the same lubricant without nanoparticles (Kedzierski 2012):

$$\frac{q''_{\mathrm{np}}}{q''_{\mathrm{PL}}} = 1 + \frac{1.45 \times 10^{-9}[\mathrm{s \cdot m^{-1}}]\left.\frac{N_{\mathrm{np}}}{A_s}\right|_{\mathrm{G}} \sigma \nu_L \rho_v x_b}{D_{\mathrm{np}}\left(q''_n\right)^{3/2} \rho_L \left(\rho_{\mathrm{np}} - \rho_L\right) g (1 - x_b)^2} \tag{29}$$

where q''_n is equal to q''_{PL} normalized by 1 $\mathrm{Wm^{-2}}$, i.e., $q''_n = q''_{\mathrm{PL}}/1\mathrm{Wm^{-2}}$ in order to make it nondimensional. Properties included in Eq. (29) are the neat refrigerant surface tension (σ), the neat refrigerant vapor density (ρ_v), the neat lubricant liquid density (ρ_L), the neat lubricant liquid kinematic viscosity (ν_L), and the nanoparticle density (ρ_{np}). The bulk mass fraction of the lubricant in the refrigerant is x_b. The pool boiling model above is based on the assumption that the enhancement is due to surface work on bubbles as caused by momentum transfer between growing bubbles and nanoparticles suspended within the lubricant excess layer. Both q''_{np} and q''_{PL} are based on the projected area of the boiling surface.

The parameter remaining to be described is the nanoparticle surface density $(N_{\mathrm{np}}/A_s)_G$, which is surface geometry dependent as the subscript "G" indicates. The N_{np}/A_s is obtained by calculating the entire active surface area of the evaporator (A_s) and dividing it into the total number of nanoparticles (N_{np}) charged to the evaporator, which can be obtained by assuming a spherical particle diameter of an average size. Figure 6 shows the nanoparticle surface density for three different surface geometries. For the smooth surface, $(N_{\mathrm{np}}/A_s)_G$ is equal to N_{np}/A_s. However, enhanced surfaces are not expected to have uniform bubble distribution over the entire surface due to gradients in temperature and heat flux. Consequently, geometry-dependent nanoparticle surface density expressions are required for enhanced surfaces. For example, for a rectangular-finned surface with 826 fins per meter (fpm) with overall fin-height and fin-tip-width of 0.76 mm and 0.36 mm, respectively, the expression for $(N_{\mathrm{np}}/A_s)_G$ is (Kedzierski 2012):

$$\left.\frac{N_{\mathrm{np}}}{A_s}\right|_G = 4.15 \times 10^8 \left(q''_n\right)^{2.53} \left(\frac{N_{\mathrm{np}}}{A_s}\left[\mathrm{m^{-2}}\right] \cdot 1 \times 10^{-20}\right)^{1.47} \tag{30}$$

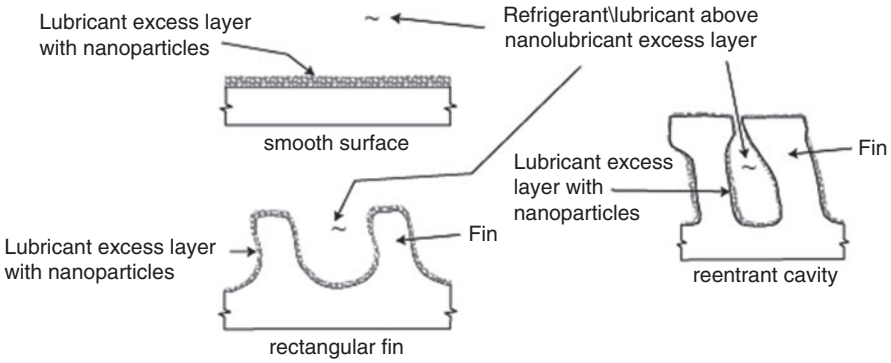

Fig. 6 Illustration of nanoparticle surface density for three surfaces

The leading constant includes the surface geometry effects for a rectangular-finned surface. For Eq. (30), the units for both $(N_{np}/A_s)_G$ and N_{np}/A_s are nanoparticles per square meter.

The nanoparticle surface density for a reentrant cavity surface reflects a greater effectiveness of the surface as compared to the rectangular-finned surface (Kedzierski 2015):

$$\left.\frac{N_{np}}{A_s}\right|_G = 4.15 \times 10^8 \left(q_n''\right)^{2.53} \left(\frac{N_{np}}{A_s}\left[\mathrm{m}^{-2}\right] \cdot 1 \times 10^{-20}\right)^{1.47} + 0.00017 q_n'' \qquad (31)$$

The additional term is a function of the normalized heat flux to account for the increased interaction between bubble and nanoparticles with increase in heat flux as more of the surface becomes active with bubble nucleation. For Eq. (31), the units for both $(N_{np}/A_s)_G$ and N_{np}/A_s are nanoparticles per square meter.

9 Pool Boiling with Additives

9.1 Additives for Boiling Water

Wasekar and Manglik (1999) review nucleate boiling enhancements with additives that work to reduce the surface tension of water. They postulate that boiling enhancement can occur with the addition of additives due to the reduction in the surface tension, while boiling degradation can occur due to the reduction in the bubble contact angle. Because both the surface tension and the contact angle decrease with the increase in the additive concentration, the result can be a negligible boiling enhancement.

Wen and Wang (2002) were able to predict the effect of the additive that they studied with the Mikic–Rohsenow (1969) model by replacing the active site density

expression with one that reflected its increase as due to surface tension reduction. The site density correlation (n_a) of Wen and Wang (2002) was:

$$n_a = C\left(\frac{1}{r_c}\right)^m (1 - \cos\Theta) \tag{32}$$

where r_c is the critical site radius for bubble nucleation, Θ is the bubble contact angle, and C and m are fitting constants that are specific to the additive. For example, Wen and Wang (2002) found the constants C and m to be 5×10^5 and 6, respectively, for one commercial surfactant.

9.2 Additives for Boiling Refrigerant

Kedzierski (2007) has shown that lubricant-based refrigerant additives can either improve refrigerant/lubricant pool boiling by as much as 95% or have essentially no effect. In this study, lubricant excess surface density measurements along with surface tension measurements and other surface chemistry analysis were done to support the opinion that the additive can form a monolayer between the wall and the lubricant/additive excess layer if the lubricant and additive are sufficiently dissimilar chemically. The general conclusion was that for an enhancement mechanism to occur, the additive must be more viscous than the existing chiller lubricant and reside at the immediate wall in a monolayer. It was also hypothesized that a monolayer will not form if the additive and the refrigerant oil are too chemically similar, e.g., both naphthenic based or both synthetic based. For this case, represented as system 1 in Fig. 7, the additive will have little influence on the refrigerant/lubricant pool boiling because it remains well mixed in the excess layer with the lubricant and is typically only 2% by mass fraction of the lubricant charge.

For system 2 to exist, it must evolve from system 1. The evolution can occur spontaneously only if the change from system 1 to system 2 results in a reduction of

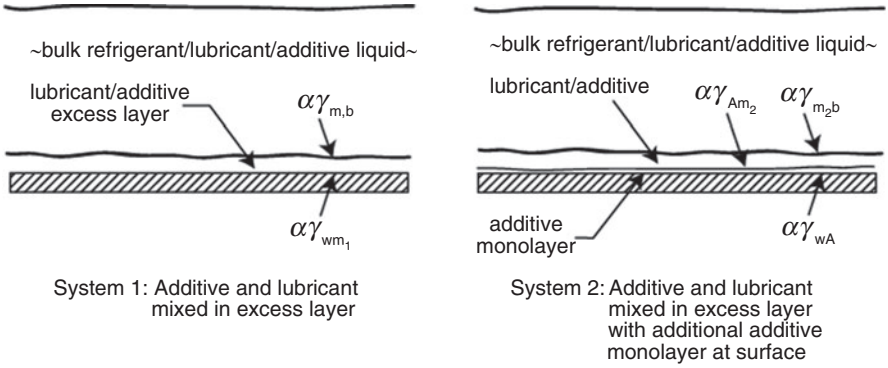

Fig. 7 Two possible surface energy systems for the refrigerant/lubricant/additive mixture

system surface energy (Rosen 1978). The requirement for system 2 to exist can be expressed in terms of surface energies by applying the analysis of spreading coefficients given by Rosen (1978):

$$a\gamma_{m_2 b} + a\gamma_{Am_2} + a\gamma_{wA} < a\gamma_{wm_1} + a\gamma_{m_1 b} \tag{33}$$

Here, a is the surface area and $\gamma_{m_2 b}$ is the interfacial free (surface) energy per unit area at the lubricant/additive mixture 2 – bulk refrigerant/lubricant/additive mixture interface. Similarly, γ_{Am_2}, γ_{wA}, γ_{wm_1}, and $\gamma_{m_1 b}$ are the surface energies of the additive – lubricant/additive mixture 2, the wall – additive, the wall – lubricant/additive mixture 1, and the lubricant/additive mixture 1 – bulk refrigerant/lubricant/additive interfaces, respectively. Subscripts 1 and 2 on the lubricant–additive mixture represent slightly different compositions of the two excess layers to account for some loss of additive to the monolayer in system 2.

By assuming that the additive monolayer does not significantly deplete the lubricant/additive excess layer of additive, $\gamma_{m_1 b}$ and $\gamma_{m_2 b}$ are approximately equal for the two systems. Many of the additive and the lubricant/additive mixture fluid properties are similar because they are essentially both lubricants. By neglecting the surface energy between the additive and the lubricant/additive mixture and using Young's equation (Adamson and Gast 1997) to quantify the surface energies associated with the additive and the lubricant, Eq. (33) simplifies to:

$$\gamma_{\mathrm{Av}} > \gamma_{\mathrm{Lv}} \tag{34}$$

Equation 34 shows that the requirement for a pure additive monolayer to exist at the surface is that the liquid–vapor surface tension of the additive is greater than that of the existing lubricant.

In summary, for a boiling enhancement to be possible with a lubricant-based additive, the following three criteria must be satisfied: (1) Eq. (34) is true; (2) the additive and lubricant are chemically dissimilar; and (3) the viscosity of the additive must be larger than the lubricant viscosity. The first two requirements make it possible for the additive to be immediately on the boiling surface. The third requirement provides the boiling enhancement by increasing the lubricant viscosity at the wall (Kedzierski 2001).

10 Cross-References

- ▶ Boiling and Two Phase flow in Narrow Channels
- ▶ Boiling in Reagent and Polymeric Solutions
- ▶ Boiling on Enhanced Surfaces
- ▶ Boiling with Nano Particles
- ▶ Flow Boiling in Tubes
- ▶ Fundamental Equations for Two Phase Flow and Heat Transfer in Tubes
- ▶ Nucleate Pool Boiling

References

Adamson AW, Gast AP (1997) Physical chemistry of surfaces, 6th edn. Interscience Publishers, New York, p. 11

Barber J, Brutin D, Tadris L (2011) A review on boiling heat transfer enhancement with nanofluids. Nanoscale Res Lett 6:280

Bigi AAM, Cremaschi L (2016) A comparison between recent experimental results and existing correlations for microfin tubes for refrigerant and nanolubricants mixtures two phase flow boiling. 16th international refrigeration and air conditioning conference, Purdue, 11–14 July, paper 2340

Bigi AMA, Wong T, Deokar P, Cremaschi L (2015) Experimental investigation on heat transfer and thermophysical properties of mixtures of Al2O3 nanolubricants and refrigerant R410A. 2015 ASHRAE Transactions, ASHRAE conference paper no. 15714, ASHRAE Winter Conference, Chicago, IL, 24–28 Jan

Brown JS (2013) Fourth ASHRAE/NIST refrigerants Conference: "moving towards sustainability". HVAC&R Research 19(2):101–102

Chaddock JB, Mathur AP (1980) Heat transfer to oil-refrigerant mixtures evaporating in tubes. 2nd multiphase flow and heat transfer symposium, Clean Energy Research Institute, University of Miami, April 1979; published in Multiphase transport: fundamentals, reactor safety, applications, Hemisphere, Washington, pp. 861–884

Chen JC (1966) Correlation for boiling heat transfer to saturated fluids in convective flow. I&EC Process Design and Development 5(3):322–329

Choi JY, Kedzierski MA, Domanski PA (2001) Generalized pressure drop correlation for evaporation and condensation in smooth and micro-fin tubes, IIF-IIR Commission B1, Paderborn, pp. B4.9–B4.16

Clift R, Grace JR, Weber ME (1979) Bubbles, drops, and particles. Academic Press, NY, p. 20

Cooper MG (1984) Saturation nucleate pool boiling- a simple correlation. Department of Engineering Science, Oxford University, England 86:785–793

Cremaschi L, Hwang Y, Radermacher R (2005) Experimental investigation of oil retention in air conditioning systems. Int J Refrig 28(7):1018–1028

Cremaschi L, Wong T, Bigi AAM (2014) Thermodynamic and heat transfer proprieties of Al2O3 nanolubricants. 15th international refrigeration and air conditioning conference at Purdue, paper no 2463, 14–17 July, West Lafayette, IN. Available online at: http://docs.lib.purdue.edu/cgi/viewcontent.cgi?article=2499&context=iracc

Cremaschi L, Bigi AAM, Wong T, Deokar P (2015) Thermodynamic properties of Al2O3 nanolubricants: part 1, effects on the two phase pressure drop. Sci Technol Built Environ, 21: 607–620, doi:10.1080/23744731.2015.1023165 (online), ISSN: 2374-4731 print / 2374-474X online

Cremaschi L, Molinaroli L, Andres C (2016) Experimental analysis and modeling of lubricant effects in microchannel evaporators working with low global warming potential refrigerants. Sci Technol Built Environ 22: 1–14, doi:10.1080/23744731.2016.118865, ISSN: 2374-4731 print / 2374-474X online

Deokar P, Cremaschi L, Wong T, Criscuolo G (2016) Effect of nanoparticles aspect ratio on the two phase flow boiling heat transfer coefficient and pressure drop of refrigerant and nanolubricants mixtures in a 9.5 mm micro-fin tube. Proceedings of the 16th international refrigeration and air conditioning conference at Purdue University, West Lafayette, IN, 11–14 July, paper no. 2098, pp. 1–10

Hamilton RL, Crosser OK (1962) Thermal conductivity of heterogeneous two-component systems. Ind Eng Chem Fundamen 1(3):187–191

Hamilton LJ, Kedzierski MA, Kaul MP (2008) Horizontal convective boiling of pure and mixed refrigerants within a micro-fin tube. J Heat Transf 15(3):211–226

Incropera FP, DeWitt DP (2002) Fundamentals of heat and mass transfer, 5th edn. John Wiley & Sons, New York

Jung DS, McLinden M, Radermacher R (1989) Measurement techniques for horizontal flow boiling heat transfer with pure and mixed refrigerants. Exp Heat Transf 2:237–255
Kedzierski MA (2001) The effect of lubricant concentration, miscibility and viscosity on R134a pool boiling. Int J Refrig 24(4):348–366
Kedzierski MA (2002) Use of fluorescence to measure the lubricant excess surface density during pool boiling. Int J Refrig 25:1110–1122
Kedzierski MA (2003a) A semi-theoretical model for predicting R123/lubricant mixture pool boiling heat transfer. Int J Refrig 26:337–348
Kedzierski MA (2003b) Improved thermal boundary layer parameter for semi-theoretical refrigerant/lubricant pool boiling model. Proceedings of international congress of refrigeration, ICR0504, Washington, DC
Kedzierski MA (2007) Effect of refrigerant oil additive on R134a and R123 boiling heat transfer performance. Int J Refrig 30:144–154
Kedzierski MA (2011) Effect of Al2O3 Nanolubricant on R134a pool boiling heat transfer. Int J Refrig 34(2):498–508
Kedzierski MA (2012) R134a/AlO Nanolubricant mixture pool boiling on a rectangular finned surface. ASME J Heat Transf 134:121501
Kedzierski MA (2013) Viscosity and density of aluminum oxide nanolubricant. Int J Refrig 36(4):1333–1340
Kedzierski MA (2015) Effect of concentration on R134a/Al2O3 Nanolubricant mixture boiling on a reentrant cavity surface. Int J Refrig 49:36–38
Kedzierski MA, Goncalves JM (1999) Horizontal convective condensation of alternative refrigerants within a micro-fin tube. J Heat Transf 6(2–4):161–178
Kedzierski MA, Gong M (2009) Effect of CuO Nanolubricant on R134a pool boiling heat transfer. Int J Refrig 25:1110–1122
Kedzierski MA, Kang DY (2016) Horizontal convective boiling of R448A, R449A, and R452B within a micro-fin tube. Sci TechnolBuilt Environ 22(8):1090–1103. doi:10.1080/23744731.2016.1186460
Kedzierski MA, Kim JH, Didion DA (1992) In: Kim JH, Nelson RA, Hashemi A (eds) Causes of the apparent heat transfer degradation for refrigerant mixtures, two-phase flow and heat transfer, vol 197. HTD, ASME, New York, pp. 149–158
Kedzierski MA, Brignoli R, Quine K, Brown JS (2016) Viscosity, density, and thermal conductivity of aluminum oxide and zinc oxide Nanolubricants. Int J Refrig 74:3–11. doi:10.1016/j.ijrefrig.2016.10.003
Laesecke A (2002) Private communications. NIST, Boulder
Lemmon EW, Huber ML, McLinden MO (2013) NIST Standard Reference Database 23, Version 9.1. Private Communications with McLinden, National Institute of Standards and Technology, Boulder
Maxwell JC (1954) A treatise on electricity and magnetism, vol 1, 3rd edn. Dover, New York, p. 440
Mikic BB, Rohsenow WM (1969) A new correlation of pool boiling data including the effect of heating surface characteristics. J Heat Transf 83:245–250
Radermacher R, Cremaschi L, Schwentker RA (2006) Modeling of oil retention in the suction line and evaporator of air conditioning systems. HVAC & R Research Journal 12(1):35–56
Reid RC, Prausnitz JM, Sherwood TK (1977) The properties of gases and liquids, 3rd edn. McGraw-Hill, New York, p. 460
Rosen MJ (1978) Surfactants and interfacial phenomena. John Wiley & Sons, New York, p. 57
Sawant NN, Kedzierski MA, Brown JS (2007) Effect of lubricant on R410A horizontal flow boiling. NISTIR 7456. U.S. Department of Commerce, Washington, D.C.
Schluender EU (1983) Heat transfer in nucleate boiling of mixtures. Int Chem Eng 23(4):589–599
Shock RAW (1982) Boiling in multicomponent fluids. In: Multiphase Science and Technology, vol 1. Hemisphere Publishing Corporation, New York, pp. 281–386

Thome JR (1989) Prediction of the mixture effect on boiling in vertical thermosiphon reboilers. Heat Transf Eng 12(2):29–38
Thome JR (1990) Enhanced boiling heat transfer. Hemisphere Publishing Corporation, Washington, D.C.
Thome JR (1995) Comprehensive thermodynamic approach to modeling refrigerant-lubricating oil mixtures. Int J HVAC&R Res 1(2):110–126
Thome JR (1999) Flow boiling inside microfin tubes: recent results and design methods. In: Kakac S et al (eds) Heat transfer enhancement of heat exchangers, Series E: applied sciences, vol 355. Kluwer Academic Publishers, Dordrecht, pp. 467–486
Tipler PL (1978) Modern physics. Worth Pub, New York, p. 320
Wasekar VM, Manglik RM (1999) A review of enhanced heat transfer in nucleate pool boiling of aqueous surfactant and polymeric solutions. J Enhanced Heat Transf 6:135–150
Wen DS, Wang BX (2002) Effects of surface wettability on nucleate pool boiling heat transfer for surfactant solutions. Int J Heat Mass Transf 45:1739–1747
Zou X, Gong MQ, Chen GF, Sun ZH, Zhang Y, Wu JF (2010) Experimental study on saturated flow boiling heat transfer of R170/R290 mixtures in a horizontal tube. Int J Refrig 33(2):371–380